Journal of Power Sources 182 (2008) 18–23

Contents lists available at ScienceDirect

Journal of Power Sources

journal homepage: www.elsevier.com/locate/jpowsour

Development of tellurium-modified carbon catalysts for oxygen reduction reaction in PEM fuel cells

Xuguang Li, Lingyun Liu, Jong-Won Lee, Branko N. Popov*

Center for Electrochemical Engineering, Department of Chemical Engineering, University of South Carolina, Columbia, SC 29208, USA

ARTICLE INFO

Article history:
Received 4 February 2008
Received in revised form 4 April 2008
Accepted 7 April 2008
Available online 14 April 2008

Keywords:
Tellurium
Carbon catalyst
Oxygen reduction
Polymer electrolyte membrane fuel cell

ABSTRACT

Tellurium (Te)-modified carbon catalyst for oxygen reduction reaction was prepared through chemical reduction of telluric acid followed by the pyrolysis process at elevated temperatures. The catalyst was found to be active for oxygen reduction reaction. High-temperature pyrolysis plays a crucial role in the formation of the active sites of the catalysts. When the pyrolysis was conducted at 1000 °C, the catalyst exhibited the onset potential for oxygen reduction as high as 0.78 V vs. NHE and generated less than 1% H_2O_2 during oxygen reduction. The performance of the membrane–electrode assembly prepared with the Te-modified carbon catalyst was also evaluated.

1. Introduction

Platinum and its alloys supported on porous carbons are the most commonly used cathode electrocatalysts for polymer electrolyte membrane (PEM) fuel cells, since they show the lowest overpotential and the highest stability among the metal catalysts. However, Pt is an expensive noble metal with low abundance, and it is thus of great interest to find low-cost alternatives for PEM fuel cells [1–3]. In this respect, much attention has been paid to transition metal chalcogenide compounds, e.g., Ru-based chalcogenides such as $Mo_4Ru_2X_8$ and RuX_y (X = S, Se and Te), since they exhibit a significant catalytic activity for oxygen reduction in acidic media [4–16].

Chalcogen elements such as S, Se and Te in the transition metal chalcogenide compounds are known to have the positive effect on the performance (activity, selectivity and stability) of catalysts for oxygen reduction. In the case of amorphous RuX_y catalysts, the chalcogen elements facilitate the catalytic oxygen reduction by serving as a bridge to transfer electrons between the Ru/carbido/carbonyl complex and the colloidal Ru nanoparticle [16]. Also, the surface modification of the Ru-based catalyst by the chalcogen elements increases the resistance to electrochemical oxidation of interfacial Ru atoms [8]. For instance, Se in the $RuSe_y$ cluster occupies electro-crystallization sites for Ru oxide formation, thereby increasing the oxidation resistance. Se atoms change the electronic nature of the cluster in such a way that favorable electronic states for oxygen reduction are formed between Se 4p and Ru 4d orbitals in the molecular cluster [9].

Carbon has a long history as a support in the heterogeneous catalysis [17]. Recent experimental studies [18–24] have demonstrated that some nitrogen-doped carbon particles show catalytic activities towards NO_x oxidation/reduction and O_2 reduction. These properties have been attributed to electronic or structural changes caused by the nitrogen incorporation into the graphite layers. At the University of South Carolina, highly active and stable metal-free carbon catalysts have been developed for PEM fuel cells [25]. They were synthesized through surface modification of porous carbon blacks with different functional groups such as oxygen and nitrogen, followed by pyrolysis and chemical activation processes. The introduction of surface functional groups decreases the activation overpotential for oxygen reduction by ca. 500 mV and the amount of H_2O_2 to a level less than 3%, in comparison to the as-received carbon black. Given the positive effect of the chalcogen elements on the oxygen reduction activities of the metal catalysts, it would be interesting to synthesize carbon-based catalysts modified by chalcogen elements and to study their electrocatalytic properties for oxygen reduction.

This paper reports a method to synthesize a tellurium-modified carbon catalyst through a chemical reduction of telluric acid followed by the pyrolysis at elevated temperatures. The catalysts were subjected to extensive materials characterization studies including X-ray diffractometry (XRD), transmission electron microscopy (TEM), and X-ray photoelectron spectroscopy (XPS). The electrocatalytic properties for oxygen reduction were evaluated using a

* Corresponding author. Tel.: +1 803 777 7314; fax: +1 803 777 8265.
E-mail address: popov@engr.sc.edu (B.N. Popov).

0378-7753/$ – see front matter © 2008 Elsevier B.V. All rights reserved.
doi:10.1016/j.jpowsour.2008.04.017

rotating ring-disk electrode (RRDE) in an acidic solution and a PEM fuel cell.

2. Experimental

2.1. Catalyst preparation

A desired amount of telluric acid ($H_2TeO_4{\cdot}H_2O$, 99.99%, Alfa Aesar) was dissolved in deionized water, followed by the addition of the carbon black (Ketjen Black EC 300J) under stirring conditions. A reducing agent, hydrazine monohydrate ($N_2H_4{\cdot}H_2O$, Aldrich) was added into the solution. The reaction mixture was refluxed at 85 °C for 12 h and then dried in a rotary evaporator at 90 °C under vacuum. The dried powder sample was heat-treated (pyrolized) at various temperatures ranging from 200 to 1100 °C in an argon atmosphere for 1 h.

2.2. Materials characterizations

In order to identify the crystal structures of the catalysts, XRD patterns were recorded with an automated Rigaku diffractometer using Cu Kα radiation over the scanning angle range of 20–50° at the scan rate of 2° min^{-1}. TEM was performed using a JEOL 2100F TEM system. The chemical analysis of the catalyst surface was performed by XPS. Measurements were carried out with a Kratos AXIS 165 high-performance electron spectrometer using a monochromatic Al Kα radiation. Low-resolution survey scans were conducted with a step size of 0.5 eV and a dwell time of 100 ms. Next, high-resolution scans were acquired in Te 3d5/2 using a 0.1 eV step size and a 300 ms dwell time.

2.3. Rotating ring-disk electrode (RRDE) measurements

Electrochemical characterizations were performed in a single-compartment, three-electrode cell using a bipotentiostat (Pine Instruments). An RRDE with a Pt ring (5.52 mm inner-diameter and 7.16 mm outer-diameter) and glassy carbon disk (5.0 mm diameter) was used as the working electrode. The catalyst ink was prepared by blending the catalyst powder (24 mg) with isopropyl alcohol (3 mL) in an ultrasonic bath. 15 μL of the catalyst ink was deposited onto the glassy carbon disk. After drying, 5 μL of Nafion solution (0.25 wt.% Nafion) was added on top of the catalyst layer to ensure better adhesion of the catalyst on the glassy carbon substrate. A platinum mesh and an Hg/Hg_2SO_4 electrode were used as the counter and reference electrodes, respectively. 0.5 M H_2SO_4 solution was used as the electrolyte. All potentials in this work were referred to a normal hydrogen electrode (NHE).

Initially, the solution was purged with nitrogen and cyclic voltammograms (CVs) were recorded by scanning the disk potential from 1.04 to 0.04 V vs. NHE at a scan rate of 5 mV s^{-1}. CVs recorded at 5 mV s^{-1} in nitrogen was used to obtain the background capacitive currents. Next, the electrolyte was purged with oxygen for 15 min. The linear sweep voltammograms were recorded at different rotation speeds of the RRDE. The oxygen reduction current was taken as the difference between currents measured in the nitrogen- and oxygen-saturated electrolytes. The ring potential was maintained at 1.2 V vs. NHE to oxidize H_2O_2 produced during oxygen reduction.

2.4. PEM fuel cell testing

The cathode catalyst ink was prepared by ultrasonically blending 0.2 g of Te/C catalyst powder with Nafion solution (5 wt.%) and isopropyl alcohol for 4 h. The catalysts ink was then sprayed onto a gas diffusion layer (GDL) (ELAT LT 1400 W, E-TEK). The process was repeated until a total catalyst loading of 6 mg cm^{-2} have been achieved. The weight ratio of Te/C to Nafion is 3:2. A commercially available catalyzed GDL (LT140EW Low Temperature ELAT® GDE Microporous Layer, E-TEK) was used as the anode for all fuel cell tests. The anode catalyst was 30 wt.% Pt/C and the Pt loading was 0.5 mg cm^{-2}. A thin layer of Nafion (0.4 mg cm^{-2}) was coated on both the cathode and anode surfaces. The Nafion-coated anode and cathode were hot-pressed to a Nafion 112 membrane at 140 °C and at 15 atm for 3 min. The geometric area of the MEA used was 5 cm^2.

The fuel cell tests were carried out in a single cell with serpentine flow channels. Pure H_2 gas humidified at 77 °C and pure O_2 gas humidified at 75 °C were supplied to the anode and cathode compartments, respectively, with a flow rate of 150 cm^3 min^{-1}. Polarization experiments were conducted using a fully automated test station (Fuel Cell Technologies Inc.) at 75 °C.

3. Results and discussion

Fig. 1 shows the powder XRD patterns of the Te-modified carbon catalysts pyrolized at various temperatures. The XRD pattern of the as-refluxed (un-pyrolized) catalyst clearly exhibits the diffraction peaks for pure Te crystalline particles as indicated in the figure. This confirms the reductive precipitation of Te particles onto the carbon support from H_2TeO_4 with the use of hydrazine ($N_2H_4{\cdot}H_2O$). As the pyrolysis temperature increases up to 400 °C, the diffraction peaks for Te particles become sharper, indicating the growth of Te particles. Upon the pyrolysis at 600 °C and beyond, however, the Te diffraction peaks are no longer observed and only a broad diffraction peak from the carbon support is observed at ca. 24.5°.

Fig. 2 displays the TEM images of the un-pyrolized Te-modified carbon catalyst and the catalyst pyrolized at 1000 °C. No Te particles

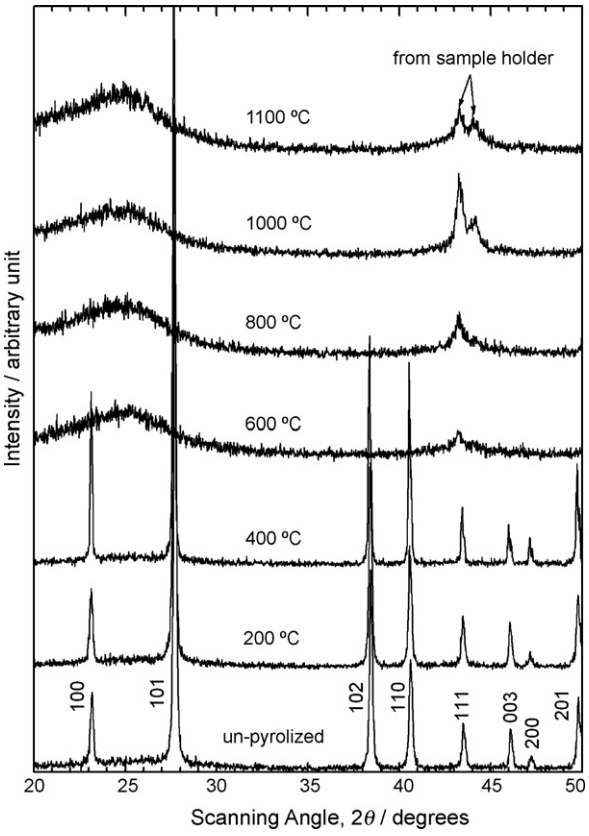

Fig. 1. Powder XRD patterns of the Te-modified carbon catalysts pyrolyzed at various temperatures.

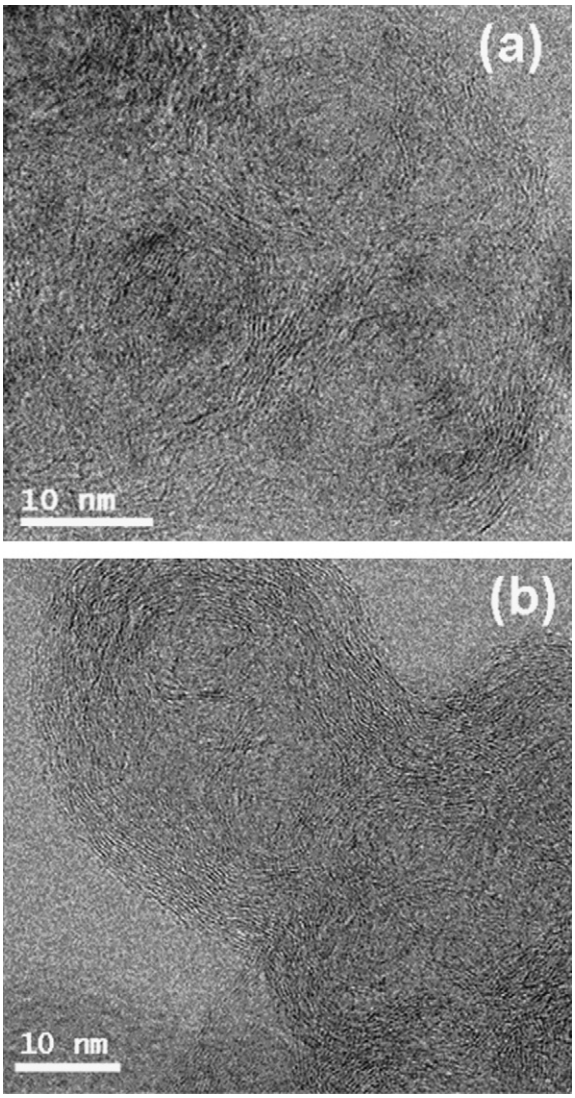

Fig. 2. TEM images of Te-modified carbon catalysts: (a) un-pyrolyzed and (b) pyrolyzed at 1000 °C.

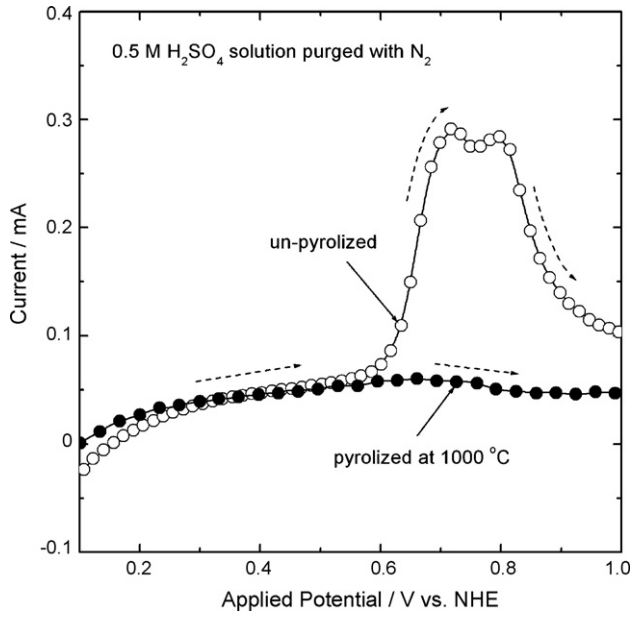

Fig. 3. Linear sweep voltammograms measured for the un-pyrolyzed Te-modified carbon catalyst and the catalyst pyrolyzed at 1000 °C. The measurements were performed in 0.5 M H_2SO_4 solution saturated with nitrogen at the potential scan rate of 50 mV s^{-1}.

or agglomerates are present on the catalyst pyrolized at 1000 °C, while nano-sized Te particles with the particle sizes of 2–4 nm are observed from the un-pyrolized catalyst.

Fig. 3 shows the linear sweep voltammograms measured for the un-pyrolized catalyst and the catalyst pyrolized at 1000 °C. The measurements were performed using a potential scan rate of 50 mV s^{-1} in 0.5 M H_2SO_4 solution deaerated by purging with N_2. The voltammogram for the un-pyrolized catalyst exhibits the anodic peaks at 0.70–0.80 V vs. NHE, which is attributed to the dissolution of Te from the carbon support. This result is in good agreement with that of Gómez et al. [26] who reported the oxidative dissolution of Te from the Au electrode substrate in H_2SO_4 solution. On the other hand, the voltammogram for the pyrolized catalyst shows only double-layer charging currents without any dissolution peak of Te.

Fig. 4(a) plots the surface concentration of Te on the catalyst as a function of the pyrolysis temperature, determined by XPS. The un-pyrolized catalyst contains 12.3 wt.% Te, but increasing pyrolysis temperature from 400 to 600 °C causes a significant loss of Te from 9.8 to 5.0 wt.%. Fig. 4(b) presents the XPS spectra of Te 3d5/2 region for the Te-modified carbon catalysts pyrolized at different temperatures. For the un-pyrolized catalysts, the XPS spectrum shows two peaks at 573.0 and 576.2 eV that correspond to the elemental tellurium (Te^0) and oxidized tellurium (i.e., TeO_2), respectively [27]. On the other hand, a single peak is observed at ca. 574.1 eV when the catalysts are pyrolized at 600–1100 °C. It is unlikely that this peak is attributed to the oxidized tellurium species since the peak position deviates significantly from those of the commonly observed tellurium oxides (i.e., 575.5–576.9 eV) [27,28]. The peak is believed to be due to the chemical bonds of Te with the carbon that is more electronegative than Te.

Given that the melting point of pure Te is 449.5 °C, solid Te particles precipitated on the carbon support would be transformed to liquid phase and/or evaporated during pyrolysis at the temperatures above 450 °C, leading to a loss of Te species. The XRD and XPS results indicate that during high-temperature pyrolysis (>450 °C), part of Te species may be re-adsorbed onto and dispersed uniformly over the carbon support, and subsequently a physisorbed Te species is transformed into a chemisorbed one (i.e., Te–C species) [29].

Fig. 5(a) presents the polarization curves for oxygen reduction on the Te-modified carbon catalysts pyrolized at different temperatures. The measurements were conducted using a potential scan rate of 5 mV s^{-1} and a rotation rate of 900 rpm in 0.5 M H_2SO_4 solution saturated with O_2. As shown in Fig. 5(a), the un-pyrolized catalyst does not exhibit any significant activity toward oxygen reduction, indicating no formation of the active sites. The catalytic activity continues to increase with increasing pyrolysis temperature, then reaches a maximum value at 1000 °C, and slightly decreases with further increasing temperature. The polarization curve for the Te-modified carbon catalyst pyrolized at 1000 °C shows an onset potential as high as 0.78 V vs. NHE and a well-defined diffusion limiting current below 0.4 V vs. NHE. Consequently, the physical, chemical, and electrochemical characterization studies indicate that Te-modified carbon is active for oxygen reduction reaction and high-temperature pyrolysis plays a critical role in the formation of the active Te–C sites.

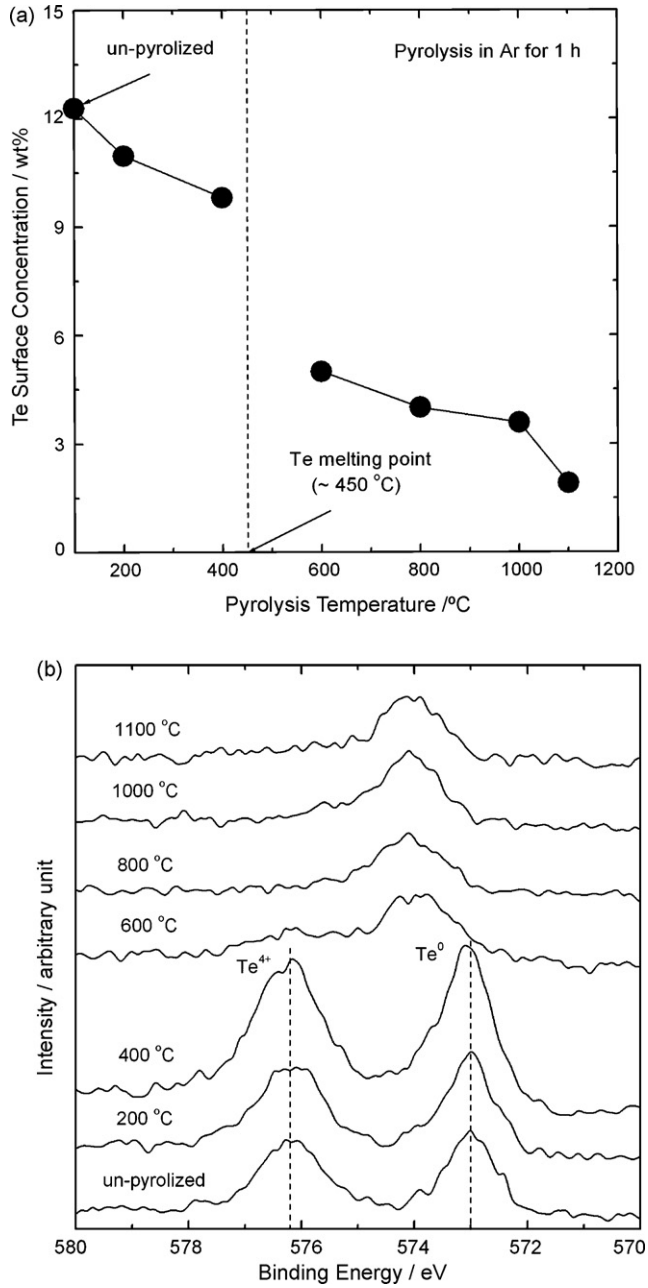

Fig. 4. (a) Surface concentration of Te on the Te-modified carbon catalysts as a function of the pyrolysis temperature and (b) XPS spectra of Te 3d5/2 region for the catalysts pyrolyzed at different temperatures.

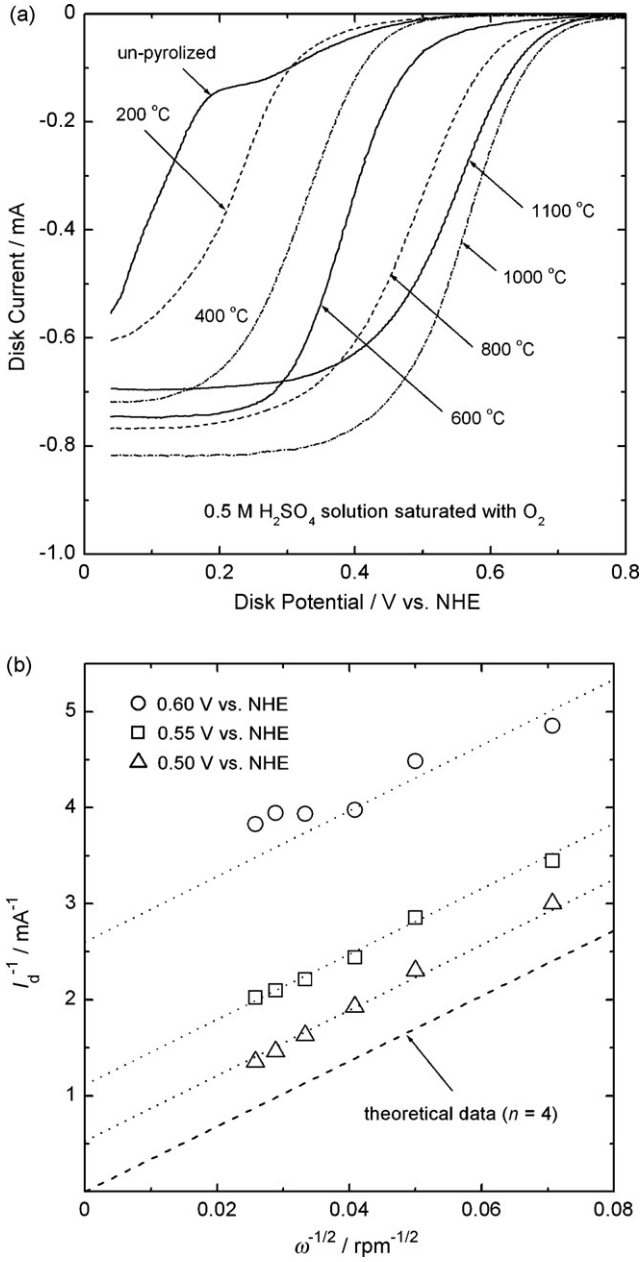

Fig. 5. (a) Polarization curves for oxygen reduction on the Te-modified carbon catalysts pyrolyzed at various temperatures and (b) Koutecky–Levich plots at 0.60, 0.55, and 0.50 V (vs. NHE) on the catalyst pyrolyzed at 1000 °C. The dashed line in (b) is the theoretical data calculated for four-electron reduction of oxygen. The RRDE measurements were performed in 0.5 M H_2SO_4 solution saturated with oxygen at the potential scan rate of 5 mV s^{-1}.

The Koutecky–Levich equation was used to calculate the kinetically limited current I_k [30]:

$$\frac{1}{I_d} = \frac{1}{I_k} + \frac{1}{I_l} + \frac{1}{I_f} = \frac{1}{nFAkC_{O_2}} + \frac{1}{0.62nFAD_{O_2}^{2/3}\omega^{1/2}\nu^{-1/6}C_{O_2}} + \frac{L}{nFAC_fD_f} \quad (1)$$

where I_d is the measured disk current, I_l the diffusion limited current, I_f the Nafion film diffusion limited current, n the number of electron exchanged in the electrochemical reaction, F the Faraday constant, A the geometric surface area of electrode, C_{O_2} the bulk concentration of oxygen, D_{O_2} the diffusion coefficient of oxygen in the bulk solution, ω the rotation rate in rpm, ν the kinematic viscosity of the solution, L the Nafion film thickness, C_f the reactant concentration in the Nafion film and D_f means the diffusion coefficient of oxygen in the Nafion film. Since the Nafion film thickness was reduced to the extent that I_f becomes significantly larger than I_k and I_l, the influence of I_f on the measured current in our experiments was negligible.

The Koutecky–Levich plots obtained at the potential range between 0.5 and 0.6 V vs. NHE are presented in Fig. 5(b) for the catalyst pyrolized at 1000 °C. A linear relationship between I_d^{-1} and $\omega^{-1/2}$ is observed and the slope remains nearly constant, regardless of the potential, which indicates that the electrochemical reaction follows first-order kinetics [5,31,32]. The dashed line

Table 1
Kinetically limited currents I_k and the amounts of H_2O_2 produced at 0.6 V vs. NHE during oxygen reduction on the Te-modified carbon catalysts pyrolized at different temperatures

Pyrolysis temperature (°C)	I_k (mA)	$\%H_2O_2$
600	0.02	11.6
800	0.09	7.6
1000	0.37	0.6
1100	0.23	1.1

in Fig. 5(b) represents the theoretical data calculated from Eq. (1) by taking the following values: $I_k = \infty$, $D_{O_2} = 1.7 \times 10^{-5}\,cm^2\,s^{-1}$, $v = 0.01\,cm^2\,S^{-1}$, $C_{O_2} = 1.3 \times 10^{-6}\,mol\,cm^{-3}$ and $n = 4.0$ (i.e., four-electron transfer). The experimental Koutecky–Levich plots exhibit the almost same slope to that of the theoretical plot, which confirms that oxygen reduction on the Te-modified carbon catalyst proceeds via the four-electron transfer pathway in acidic environment.

Table 1 summarizes the kinetically limited current I_k and the amount of H_2O_2 produced during oxygen reduction, respectively, as a function of the pyrolysis temperature. The value of I_k was determined from the y-intercept of the $I_d{}^{-1}$ vs. $\omega^{-1/2}$ plot in Fig. 5(b), and $\%\,H_2O_2$ was estimated using the following equation [30]:

$$\%H_2O_2 = \frac{200\ I_r/N}{I_d + I_r/N} \quad (2)$$

where I_r is the ring current, and N represents the collection efficiency. Here, the value of N was taken as 0.39. The measurements were conducted at 0.6 V vs. NHE. As the pyrolysis temperature increases from 600 to 1000 °C, the I_k value increases from 0.02 to 0.37 mA, and at the same time the amount of H_2O_2 produced during oxygen reduction drops from 11.6% to 0.6%. The pyrolysis at 1100 °C results in a slight decrease of the catalytic activity and selectivity due to very low concentration of Te–C sites as indicated in Fig. 4(a). It is generally known that a carboneous material catalyzes oxygen reduction to H_2O_2 via two-electron pathway; however, the carbon modification through Te deposition from H_2TeO_4 followed by pyrolysis facilitates four-electron oxygen reduction to water.

Fig. 6 shows the polarization curves of the PEM fuel cells with the Te-modified carbon catalyst. The catalyst was prepared by pyrolysis at 1000 °C. The cathode catalyst loading in the MEA was 6 mg cm^{-2} and the fuel cell testing was performed at 75 °C using H_2 and O_2. The open circuit potential of the MEA was measured to be approximately 0.76 V. When the fuel cell was operated at ambient pressure, the current density is ca. 0.89 A cm^{-2} at 0.2 V and the maximum power density is approximately 0.19 W cm^{-2}. When the fuel cell was operated at the back pressures of 30 psi for both anode and cathode, the current density is approximately 1.26 A cm^{-2} at 0.2 V and the maximum power density is approximately 0.27 W cm^{-2}.

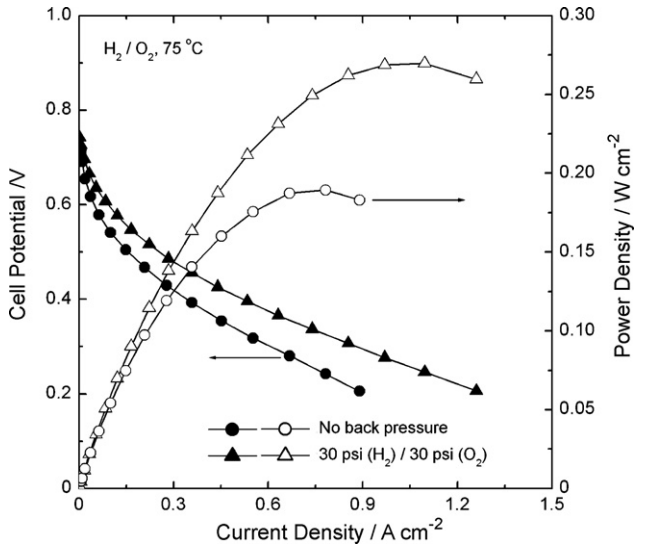

Fig. 6. Polarization curves of the PEM fuel cells with the Te-modified carbon catalyst pyrolyzed at 1000 °C in the absence and presence of H_2/O_2 back pressure. Anode catalyst loading: 0.5 mg Pt cm^{-2}; cathode catalyst loading: 6.0 mg cm^{-2}; H_2 and O_2 flow rates: 150 cm^3 min^{-1}.

4. Conclusions

Te-modified carbon catalysts for oxygen reduction were synthesized by chemical reduction of telluric acid followed by the pyrolysis process at elevated temperatures. The XPS and RRDE studies indicated that high-temperature pyrolysis has a crucial role in the formation of the active sites of catalysts for oxygen reduction. The catalyst pyrolized at 1000 °C exhibited the onset potential for oxygen reduction as high as 0.78 V vs. NHE and generated less than 1% H_2O_2 during oxygen reduction. The PEM fuel cell showed the current density of ca. 1.26 A cm^{-2} at 0.2 V and the maximum power density of ca. 0.27 W cm^{-2} when it was run with the back pressures of 30 psi for both anode and cathode.

Acknowledgement

Financial support provided by the Department of Energy (DOE) is acknowledged gratefully.

References

[1] J.P. Dodelet, in: J.H. Zagal, F. Bedioui, J.P. Dodelet (Eds.), N4-Macrocyclic Metal Complexes, Springer, New York, 2006, p. 3.
[2] N.P. Subramanian, S.P. Kumaraguru, H. Colon-Mercado, H. Kim, B.N. Popov, T. Black, D.A. Chen, J. Power Sources 157 (2006) 56–63.
[3] R. Bashyam, P. Zelenay, Nature 443 (2006) 163–166.
[4] N. Alonso-Vante, H. Tributsch, Nature 323 (1986) 431–432.
[5] N. Alonso-Vante, W. Jaegermann, H. Tributsch, W. Hönle, K. Yvon, J. Am. Chem. Soc. 109 (1987) 3251–3257.
[6] N. Alonso-Vante, H. Tributsch, O. Solorza-Feria, Electrochim. Acta 40 (1995) 567–576.
[7] I.V. Malakhov, S.G. Nikitenko, E.R. Savinova, D.I. Kochubey, N. Alonso-Vante, J. Phys. Chem. B 106 (2002) 1670–1676.
[8] M. Bron, P. Bogdanoff, S. Fiechter, I. Dorbandt, M. Hilgendorff, H. Schulenburg, H. Tributsch, J. Electroanal. Chem. 500 (2001) 510–517.
[9] F. Dassenoy, W. Vogel, N. Alonso-Vante, J. Phys. Chem. B 106 (2002) 12152–12157.
[10] A. Lewera, J. Inukai, W.P. Zhou, D. Cao, H.T. Duong, N. Alonso-Vante, A. Wieckowski, Electrochim. Acta 52 (2007) 5759–5765.
[11] N. Alonso-Vante, I.V. Malakhov, S.G. Nikitenko, E.R. Savinova, D.I. Kochubey, Electrochim. Acta 47 (2002) 3807–3814.
[12] S. Fiechter, I. Dorbandt, P. Bogdanoff, G. Zehl, H. Schulenburg, H. Tributsch, M. Bron, J. Radnik, M. Fieber-Erdmann, J. Phys. Chem. C 111 (2007) 477–487.
[13] C. Fischer, N. Alonso-Vante, S. Fiechter, H. Tributsch, J. Appl. Electrochem. 25 (1995) 1004–1008.
[14] R.G. González-Huerta, J.A. Chávez-Carvayar, O. Solorza-Feria, J. Power Sources 153 (2006) 11–17.
[15] R.W. Reeve, P.A. Christensen, A.J. Dickinson, A. Hamnett, K. Scott, Electrochim. Acta 45 (2000) 4237–4250.
[16] H. Tributsch, M. Bron, M. Hilgendorff, H. Schulenburg, I. Dorbandt, V. Eyert, P. Bogdanoff, S. Fiechter, J. Appl. Electrochem. 31 (2001) 739–748.
[17] K. Kinoshita, Carbon: Electrochemical and Physicochemical Properties, John Wiley & Sons, New York, 1988.
[18] H. Wang, R. Côté, G. Faubert, D. Guay, J.P. Dodelet, J. Phys. Chem. B 103 (1999) 2042–2049.
[19] G. Lalande, R. Côté, D. Guay, J.P. Dodelet, L.T. Weng, P. Bertrand, Electrochim. Acta 42 (1997) 1379–1388.
[20] L.R. Radovic, F. Rodriguez-Reinoso, in: P.A. Thrower (Ed.), Chemistry and Physics of Carbon, vol. 25, Marcel Dekker, New York, 1997, p. 243.
[21] D. Mang, H.P. Boehm, K. Stanczyk, H. Marsh, Carbon 30 (1992) 391–398.
[22] M. Huang, H. Teng, Carbon 41 (2003) 951–957.
[23] S. Matzner, H.P. Boehm, Carbon 36 (1998) 1697–1709.
[24] B. Stöhr, H.P. Boehm, R. Schlögl, Carbon 29 (1991) 707–720.

[25] B.N. Popov, FY 2006 Annual Progress Report, DOE Hydrogen Program, V.C.2, 774–778.
[26] H. Gómez, R. Henríquez, R. Schrebler, G. Riveros, R. Córdova, Electrochim. Acta 46 (2001) 821–827.
[27] J.F. Moulder, W.F. Stickle, P.E. Sobol, K.D. Bomben, Handbook of X-ray Photoelectron Spectroscopy, PerkinElmer, Eden Prairie, MN, 1993.
[28] S.K. Chan, H.J. Liu, C.T. Chan, Z.Q. Zhang, W.K. Ge, I.K. Sou, Phys. Rev. B 71 (2005) 195421.
[29] A.L. Wijnoltz, Thesis, Eindhoven University of Technology, The Netherlands, 1995 (chapter 2).
[30] U.A. Paulus, T.J. Schmidt, H.A. Gasteiger, R.J. Behm, J. Electroanal. Chem. 495 (2001) 134–145.
[31] O. Solorza-Feria, S. Ramírez-Raya, R. Rivera-Noriega, E. Ordoñez-Regil, S.M. Fernández-Valverde, Thin Solid Films 311 (1997) 164–170.
[32] C. Paliteiro, L. Batista, J. Electrochem. Soc. 147 (2000) 3445–3455.